Available online at www.sciencedirect.com
ScienceDirect
Journal of Molecular Catalysis A: Chemical 279 (2008) 239–247
JOURNAL OF MOLECULAR CATALYSIS A: CHEMICAL
www.elsevier.com/locate/molcata

Enhanced enantioselectivity of chiral hydrogenation catalysts after immobilisation in thin films of ionic liquid

Kam Loon Fow [a], Stephan Jaenicke [a], Thomas E. Müller [a,b,*], Carsten Sievers [b]

[a] National University of Singapore, Faculty of Science, Department of Chemistry, 3 Science Drive 3, Singapore 117543, Singapore
[b] Technische Universität München, Department Chemie, Lichtenbergstrasse 4, 85747 Garching, Bayern, Germany

Available online 3 December 2006

Abstract

Chiral organometallic complexes were immobilized in silica supported thin films of ionic liquid. The heterogenized catalysts were tested in the hydrogenation of acetophenone, which was chosen as test reaction for the enantioselective reduction of prochiral ketones. High enantioselectivities (up to 74% ee) were achieved in supported ionic liquids using a catalyst/substrate pair, which showed no enantioselectivity in methanol. This is attributed to the unique solvent properties of ionic liquids including the formation of solvent cages of ionic liquid molecules around the complexes. Within these cages, transition states are modified and chemical transformations follow alternative reaction pathways.

Keywords: Hydrogenation; Ketone; Enantioselectivity; Ionic liquid; Two-phase catalysis; Immobilisation

1. Introduction

Asymmetric metal complexes are used extensively as molecular catalysts to introduce chirality during synthesis of enantiopure organic compounds [1]. In particular, noble metal complexes with chiral phosphine ligands have been reported to provide high enantio-selectivities [2]. However, in industrial applications homogeneous catalysts are often difficult to separate from the product. This problem does not arise when heterogeneous catalysts are used. Current strategies for the immobilization [3,4] of organometallic complexes include cross-linking with organic [5–7] or inorganic groups [8], fixation on solid supports (oxides [9,10], polymers [11]) or in a liquid phase [12–14]. However, enantioselectivity is frequently lost in common methods for the immobilisation of homogeneous catalysts [15,16].

The strategy adopted in this study was to immobilise organometallic complexes in a thin film of supported ionic liquid [17–23]. The aim was to combine the advantages of homogeneous and heterogeneous catalysis. As the complexes are in a highly flexible environment, we expected that the activity of the homogeneous catalysts is retained. The formation of solvent cages of ionic liquid molecules around organometallic complexes [24] might even lead to enhanced substrate–catalyst interactions. Phosphonium salts [25] were chosen for this study, as they provide a wide mixability gap with organic solvents such as hexane (mobile phase) and are compatible with the basic reaction conditions required for this study (*vide infra*) [26].

As model reaction, the stereoselective hydrogenation of a non-chelating prochiral ketone was explored. Various homogeneous catalysts are known for the enantioselective reduction of β-ketoester and other chelating ketones [27–29]. Frequently, the atropisomeric bidentate phosphine ligand (*R*)- or (*S*)-2,2′-bis(diphenylphosphino)-1,1′-binaphthyl (BINAP) is used to assemble the chiral complex [30,31]. The asymmetric hydrogenation of non-chelating ketones is more difficult. Aromatic ketones can be hydrogenated using Noyori catalysts [$RuCl_2$(diphosphine)(diamine)] [32–36] or rhodium catalysts, such as [Rh(COD)Cl]$_2$/2PennPhos [37].

The immobilisation of chiral hydrogenation catalysts of the first generation was explored in this study. As model reaction, the reduction of acetophenone was tested. The focus was on evaluating a possible selectivity enhancement compared to the corresponding homogeneous catalysis, which we expected after immobilisation of the chiral complexes in the ionic liquid.

* Corresponding author at: Technische Universität München, Department Chemie, Lichtenbergstrasse 4, 85747 Garching, Bayern, Germany.
Tel.: +49 8928912827; fax: +49 8928913544.
E-mail address: thomas.mueller@tum.de (T.E. Müller).

1381-1169/$ – see front matter © 2006 Elsevier B.V. All rights reserved.
doi:10.1016/j.molcata.2006.11.050

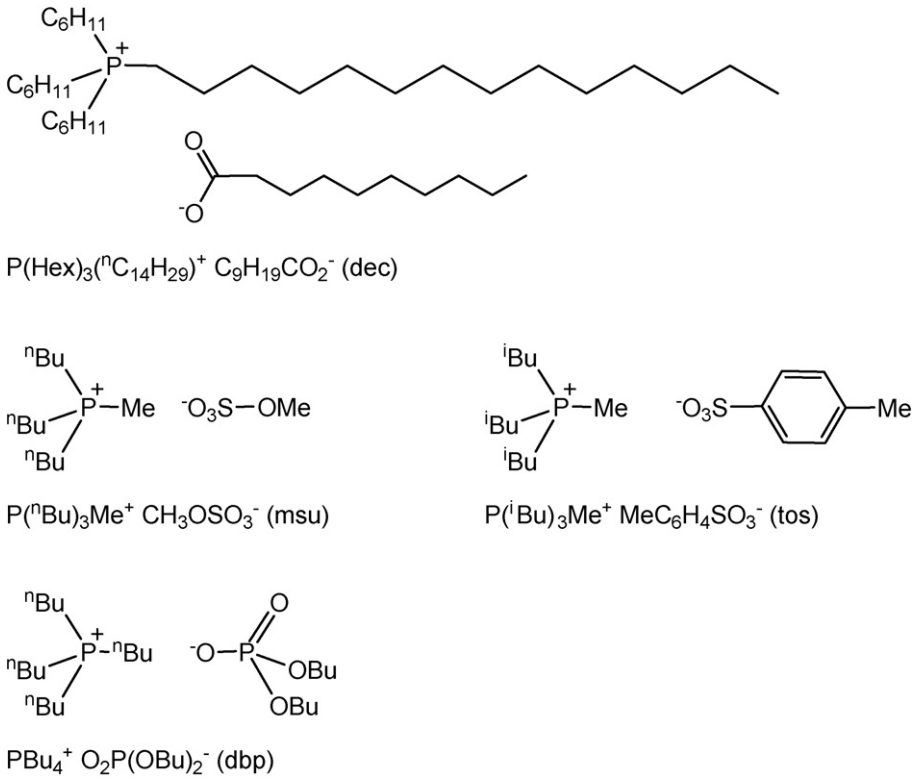

Fig. 1. Phosphonium salts used in this study.

2. Experimental

2.1. Materials

Silica beads were obtained from Degussa (Aerolyst 355, extrudates from Aerosil 200, 2.5 mm diameter, specified BET surface area 150 $m^2\,g^{-1}$, pore volume 0.84 $cm^3\,g^{-1}$). Prior to use, the silica beads were dried at 200 °C for 1 h. For preparation of catalysts containing K_2CO_3, the silica beads (25 g) were suspended in a solution of K_2CO_3 (0.43 g, 3.1 mmol) in water (35 ml). The mixture was allowed to stand for 1 h. Subsequently, the water was removed by heating for 6 h to 100 °C and for 4 h to 200 °C. For catalysts containing K_3PO_4, the same procedure was adopted using K_3PO_4 (0.66 g, 3.1 mmol) instead of K_2CO_3.

The ionic liquids triisobutyl(methyl)phosphonium tosylate (abbreviated tos, trade name CYPHOS IL 106), tributyl(methyl)phosphonium methylsulphate (msu, CYPHOS IL 108), tetrabutylphosphonium dibutylphosphate (dbp, CYPHOS IL 107) and tetradecyl(trihexyl)phosphonium decanoate (dec, CYPHOS IL 103) were obtained from Cytec Industries Inc., Canada and dried by heating in vacuum to 165 °C over night (Fig. 1). During this procedure, a compound sublimed from triisobutyl(methyl)phosphonium tosylate. TGA analysis had indicated that about 5–8 wt% of a volatile material was contained in the ionic liquid. The compound was identified as phosphine oxide $^{i}Bu_3PO$ by the single signal at 46 ppm in the $^{31}P\{^{1}H\}$ NMR spectrum.

All other reagents were obtained from Aldrich, dried and degassed prior to use and subsequently handled under inert atmosphere.

2.2. Catalyst preparation

In a typical procedure, the complex $[Rh(COD)_2]CF_3SO_3$ (59.3 mg, 0.124 mmol) was dissolved in CH_2Cl_2 (4 cm^3). A solution of (*R*)-BINAP (79.6 mg, 0.124 mmol) in CH_2Cl_2 (10 cm^3) was added slowly. The solution was stirred for 1 h. The ionic liquid $P(Hex)_3(n\text{-}C_{14}H_{29})^+$ $C_9H_{19}CO_2^-$ (1.3 g, 1.5 cm^3) and silica beads pre-treated with K_3PO_4 (10 g) were added to the solution. The mixture was allowed to stand for 1 h, and then cooled rapidly to liquid nitrogen temperature; the volatiles were removed *in vacuo*, while the mixture was warmed slowly to room temperature. Detailed procedures for all catalysts (see Table 1) are provided in supplementary data. The supported catalysts were highly sensitive to traces of oxygen and water and handled under inert atmosphere.

2.3. Physicochemical characterisation

BET surface area analyses were performed on a Micromeritics TriStar 3000 gas adsorption analyzer. All samples were degassed at 100 °C for 4 h under nitrogen flow prior to analysis. The metal content of the catalysts was determined by AAS on a UNICAM 939 spectrometer. The carbon and hydrogen content was measured on an elementar vario EL or Heraeus CHN-Rapid analyser. For MAS NMR measurements, the samples were ground and packed into 4 mm ZrO_2 rotors under inert atmosphere. A Bruker MSL300 spectrometer ($B_0 = 7.5$ T) was used. The spinning rate was 10 kHz. For the ^{1}H spectra, 64 scans were recorded with a recycle time of 2 s. The spectra were calibrated

Table 1
Supported catalysts used in this study

Name	Organometallic complex[a]	Ionic liquid	Additive
Rh/dec/PO_4	[Rh(COD)$_2$]CF_3SO_3/(*R*)-BINAP[b]	P(Hex)$_3$(*n*-$C_{14}H_{29}$)$^+$ $C_9H_{19}CO_2^-$	K_3PO_4
Rh/dbp/PO_4	[Rh(COD)$_2$]CF_3SO_3/2 equiv. (*R*)-BINAP[b]	PBu_4^+ $O_2P(OBu)_2^-$	K_3PO_4
Rh/tos/–	[Rh((*S*)-BINAP)(COD)]ClO_4·thf	P(^{i}Bu)$_3$Me$^+$ $MeC_6H_4SO_3^-$	–
Rh/tos/CO_3	[Rh((*S*)-BINAP)(COD)]ClO_4·thf	P(^{i}Bu)$_3$Me$^+$ $MeC_6H_4SO_3^-$	K_2CO_3
Rh(chi)/msu/–	[Rh((*SS*)-chiraphos)(NOR)]ClO_4	P(^{n}Bu)$_3$Me$^+$ $CH_3OSO_3^-$	–
Rh(chi)/tos/CO_3	[Rh((*SS*)-chiraphos)(NOR)]ClO_4	P(^{i}Bu)$_3$Me$^+$ $MeC_6H_4SO_3^-$	K_2CO_3
Ru/dec/PO_4	[Ru(PPh_3)$_3Cl_2$]/(*R*)-BINAP[b]	P(Hex)$_3$(*n*-$C_{14}H_{29}$)$^+$ $C_9H_{19}CO_2^-$	K_3PO_4
Ru/tos/–	$RuCl_3$/(*R*)-BINAP[b]	P(^{i}Bu)$_3$Me$^+$ $MeC_6H_4SO_3^-$	–
Ru/tos/CO_3	$RuCl_3$/(*R*)-BINAP[b]	P(^{i}Bu)$_3$Me$^+$ $MeC_6H_4SO_3^-$	K_2CO_3

[a] *Abbreviations*: (*R*)-BINAP: (*R*)-(+)-2,2′-bis(diphenylphosphino)-1,1′-binaphthyl; (*S*)-BINAP: (*S*)-(−)-2,2′-bis(diphenylphosphino)-1,1′-binaphthyl; COD: 1,5-cyclooctadiene; thf: tetrahydrofuran; (*SS*)-chiraphos: (2*S*,3*S*)-bis(diphenylphosphino)butane; NOR: 2,5-norbornadiene.
[b] In situ mixture.

against an external standard of adamantane ($\delta = 1.7$ ppm). The ^{31}P spectra were measured with proton decoupling as the sum of at least 5000 scans. Chemical shifts are reported relative to $(NH_4)H_2PO_4$ at 1.11 ppm. A summary of the analytical data and the chemical shifts in NMR is provided in supplementary data. NMR data for the parent ionic liquids and assignment of the signals are also provided in supplementary data.

2.4. Catalysis

A 300 cm^3 autoclave (Autoclave engineers or Parr) with glass or Teflon liner was charged under inert conditions with the supported catalyst (1.6 g), hexane (100 ml), undecane (100 μl) and acetophenone (194 μl, 1.66 mmol). For experiments involving homogeneous catalysts, a mixture of catalyst (0.017 mmol), K_2CO_3 (23 mg, 0.17 mmol), methanol (100 ml), undecane (100 μl) and acetophenone (194 μl, 1.66 mmol) was charged into the autoclave. The vessel was closed, purged several times with nitrogen and heated to 50 °C, if not stated otherwise. The reaction was started by pressurising the autoclave rapidly with hydrogen to a total pressure of 50 bar. Samples were taken in regular intervals and analysed with gas chromatography (GC) using an Agilent 6890N equipped with FID detector and HP-5 column. Enantiomeric excess (ee) and configuration of 1-phenylethanol were determined using a Supelco BetaDex 325 column.

3. Results and discussion

3.1. Catalyst preparation and characterisation

Rhodium and ruthenium complexes with bidentate chiral phosphines were reported as effective molecular catalysts for the enantioselective hydrogenation of ketones bearing a second coordinating group in the vicinity [32,38,39]. In this respect, we expected strongly enhanced substrate–catalyst interactions due to the unique solvent properties of ionic liquids [24]. In this study, we explored if these complexes could be used also in the reduction of simple ketones, when immobilised in thin films of supported phosphonium salts (Fig. 1). As catalysts, the rhodium complexes [Rh((*R*)-BINAP)(COD)]CF_3SO_3, [Rh((*S*)-BINAP)(COD)]ClO_4·thf, and [Rh((*SS*)-chiraphos)(NOR)]ClO_4, and the ruthenium complexes [Ru((*R*)-BINAP)(PPh_3)Cl_2] and [Ru((*R*)-BINAP)Cl_3] were chosen (Table 1). The supported catalysts were prepared by impregnation of silica with a solution of the organometallic complex and base (K_2CO_3 and K_3PO_4) [44].

The catalysts were obtained as free flowing powders, which could be handled in the same way as classic heterogeneous catalysts. Prior to testing in catalysis, the materials were characterised in detail (see Table 2). Nitrogen adsorption showed that by impregnation the total pore volume was reduced from 0.77 to 0.71–0.53 cm^3 g^{-1}, while the BET surface area did not change

Table 2
Analytical data of the supported catalysts used in this study

Material[a]	BET surface area (m^2 g^{-1})	Pore volume[b] (cm^3 g^{-1})	Carbon content (wt%)	Hydrogen content (wt%)	Concentration of ionic liquid (wt%)
Parent silica beads	141	0.77	–	–	–
Rh/dec/PO_4	120	0.60	9.22	1.82	12.0
Rh/dbp/PO_4	96	0.57	9.77	1.99	15.9
Rh/tos/–	143	0.70	10.29	1.65	16.6
Rh/tos/CO_3	102	0.69	7.82	1.27	12.7
Rh(chi)/msu/–	161	0.66	5.64	1.25	11.0
Rh(chi)/tos/CO_3	118	0.66	7.10	1.25	11.5
Ru/dec/PO_4	129	0.53	8.82	1.67	11.5
Ru/tos/–	151	0.69	6.55	1.10	10.6
Ru/tos/CO_3	147	0.64	7.61	1.27	12.3

[a] All catalysts had a metal content of 0.011 mmol g^{-1}.
[b] The volume of ionic liquid was equal for all samples (0.15 cm^3 g_{silica}^{-1}).

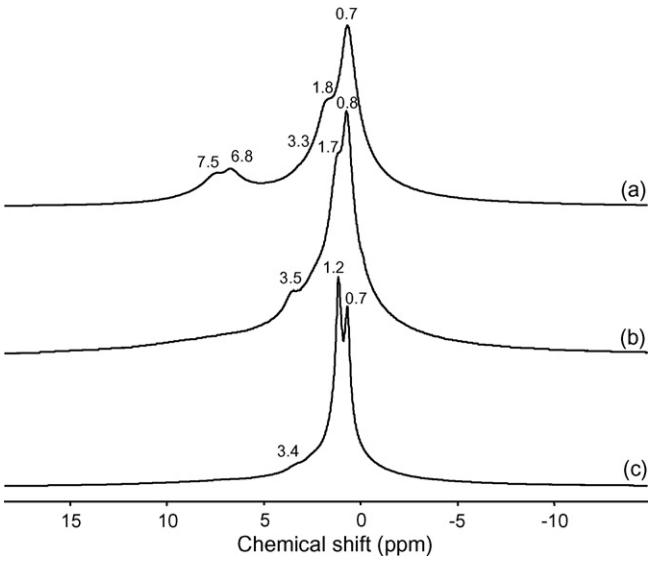

Fig. 2. ^{1}H MAS NMR spectra of supported catalysts, (a) Rh/tos/CO_3, (b) Rh/dbp/PO_4, (c) Rh/dec/PO_4.

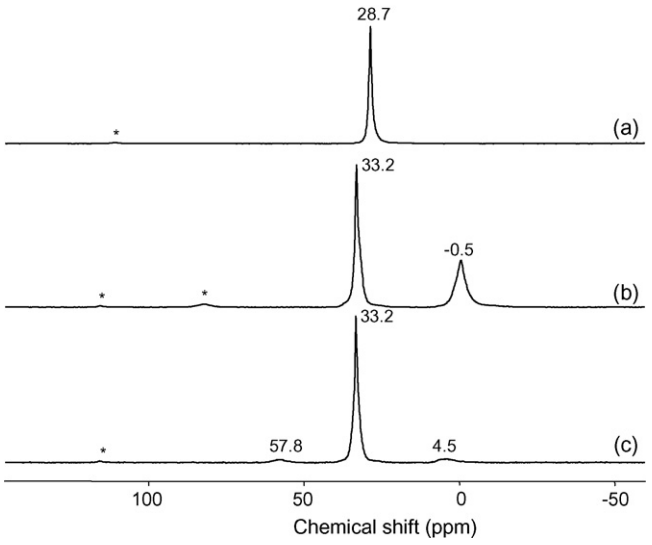

Fig. 3. ^{31}P-MAS NMR spectra of supported catalysts, (a) Rh/tos/CO_3, (b) Rh/dbp/PO_4, (c) Rh/dec/PO_4. Spinning side bands are marked with an asterisk (*).

significantly. Closer analysis of the adsorption isotherms showed that small pores with 3 nm diameter (corresponding to roughly 0.02 $cm^3\ g^{-1}$ volume) were filled entirely with the ionic liquid. The remaining ionic liquid apparently formed an even film (average thickness ~1.1 nm) on the inside of the larger pores reducing their volume by 0.04–0.22 $cm^3\ g^{-1}$. Note that the volume of ionic liquid added per gram of silica was equal for all catalysts (0.15 cm^3).

The ^{1}H MAS NMR spectra of selected catalysts are compiled in Fig. 2. The spectra are similar to those of the respective ionic liquids in $CDCl_3$ (not shown, for chemical shifts, see supplementary data). The spectra are dominated by the signals of the ionic liquid, whereas the signals of the phosphine ligands and the SiOH groups of the support were not resolved. It is particularly noteworthy that a strong line broadening was observed.

The $^{31}P\{^{1}H\}$ MAS NMR spectra of selected catalysts are shown in Fig. 3. The chemical shift was 28.7 ppm for the triisobutyl(methyl)phosphonium cation in Ru/tos/CO_3, Rh/tos/CO_3 and Rh(chi)/tos/CO_3. In the spectrum of Rh/dbp/PO_4, peaks at 33.2 and −0.5 ppm can be distinguished, which are assigned to the tetrabutylphosphonium cation and the dibutylphosphate anion of the ionic liquid, respectively. More complex spectra were obtained for the catalysts containing tetradecyl(trihexyl)phosphonium decanoate (Ru/dec/PO_4 and Rh/dec/PO_4). The peak at 33.1 ppm is assigned to the tetradecyl(trihexyl)phosphonium cation, while the signals at 57.6 and 4.3 ppm are attributed to the ligands in the complex [40] and free phosphine, respectively. All ^{31}P resonances were shifted by 0.4–0.6 ppm to higher field compared to the spectra of the ionic liquids in $CDCl_3$, which is consistent with a solvent effect caused by the different dielectric constant of the surrounding medium. Note that the dissolved complex did not influence the position of the NMR signals. Thus, direct coordination of the phosphonium salts to the metal complexes could be ruled out. As for the ^{1}H NMR spectra, a strong line broadening was observed for the ^{31}P NMR spectra of the supported ionic liquids. The line width was 134 Hz for the signal of the triisobutyl(methyl)phosphonium cation in Ru/tos/CO_3, 200 and 427 Hz for the signals of the tetrabutylphosphonium cation and the dibutylphosphate anion in Rh/dbp/PO_4, respectively, and 186 Hz for the signal of the tetradecyl(trihexyl)phosphonium cation in Rh/dec/PO_4. In contrast, the line width in the neat ionic liquids was in the range 12–21 Hz.

The line broadening is related to a reduced mobility of the ionic liquid molecules within the liquid film [24]. In NMR spectra of solids, the chemical shift anisotropy is not averaged out by the motion of the molecules, but can be removed by magic angle spinning (MAS) [41]. Differences in T2, which is not influenced by MAS, are the main reason for changes in the line-width and can be taken as a measure for the mobility of a particular atomic group [24,42]. The increase in line-width, therefore, shows that the mobility of the individual molecules was severely restricted. Strong interactions between ionic liquid and support could be excluded as the NMR signals were observed at the same chemical shift as for the neat ionic liquids. Recently, a similar effect was reported for palladium complexes dissolved in imidazolium salts and explained by formation of solvent cages of ionic liquid molecules around the complex molecules [24]. We speculate that phosphonium salts give rise to similar solvent cages, which arrange to supramolecular aggregates of 1 complex molecule and 16–33 ion pairs of the ionic liquid. The aggregates arrange into a three-dimensional regular packing with glass-like structure, in which the mobility of the ionic liquid molecules is reduced.

3.2. Reduction of acetophenone with supported catalysts

The reduction of acetophenone to (*S*) or (*R*)-1-phenylethanol (Eq. (1)) was chosen as test reaction for the enantioselective hydrogenation of aromatic ketones. A possible side reaction is the reduction of the phenyl ring, which leads to 1-cyclohexylethanone and (*S*) or (*R*)-1-cyclohexylethanol (Fig. 5).

However, for many homogeneous catalysts a high chemoselectivity for reduction of the keto group is observed [43].

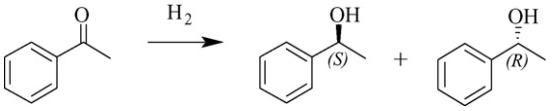

(1)

Yields in 1-phenylethanol up to 79% and enantiomeric excess up to 74% were achieved with supported rhodium catalysts. Note that no conversion was observed for catalysts, which did not contain K_2CO_3 or K_3PO_4 as additive (Rh(chi)/msu/–, Rh/tos/–, Ru/tos/–) indicating that basic reaction conditions were essential [44]. In general, high chemoselectivity to 1-phenylethanol led to low enantioselectivity to (*S*) or (*R*)-1-phenylethanol and *vice versa* (Table 3). Stereoselection was observed only for complexes containing the BINAP ligand, whereas for Rh(chi)/tos/CO_3 containing (2*S*,3*S*)-bis(diphenylphosphino)butane the enantioselectivity was negligible (2% ee at 63% conversion). The catalyst Rh/dec/PO_4 provided good chemoselectivity to 1-phenylethanol (70% at 90% conversion) and moderate enantioselectivity (30% ee). In contrast, Rh/tos/CO_3 showed low chemoselectivity (42% at 27% conversion, decreasing to 6% at 100% conversion) and relatively high enantioselectivity (74% ee at 100% conversion). Note that the enantioselectivity observed with supported catalysts is unique as no stereoselection was found in the corresponding homogeneous catalysis (*vide infra*).

Both supported ruthenium catalysts (Ru/dec/PO_4 and Ru/tos/CO_3) showed a high initial rate of reaction (0.24 and 0.21 mol_{Sub} $(mol_{Cat}\ h)^{-1}$) and moderate enantioselectivity (49–55% at 22–36% conversion). However, the catalysts deactivated rapidly. Deactivation was less pronounced in the ionic liquid $P(^iBu)_3Me^+$ $MeC_6H_4SO_3^-$ (Ru/tos/CO_3), where 36% conversion was obtained after 17 h. In contrast, in the ionic liquid $P(Hex)_3(n\text{-}C_{14}H_{29})^+$ $C_9H_{19}CO_2^-$ (Ru/dec/PO_4) the conversion was 22% after 15 h.

A typical time-concentration diagram for the supported rhodium catalysts is shown in Fig. 4 (Rh/dec/PO_4). 1-Phenylethanol was formed as the main product. In parallel, 1-cyclohexylethanone was formed in smaller concentration. At longer reaction times, the concentration of 1-cyclohexylethanone decreased, while the concentration of 1-cyclohexylethanol increased. This is clearly indicative of a secondary

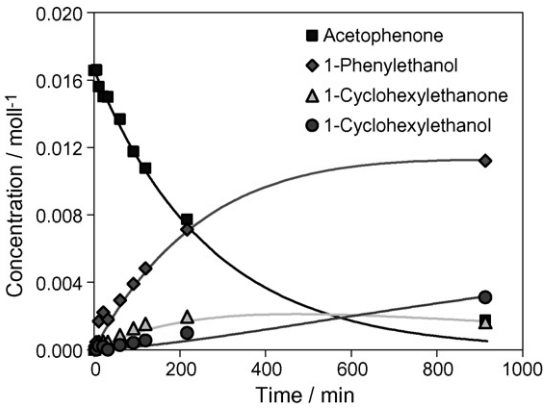

Fig. 4. Time concentration diagram for the hydrogenation of acetophenone with Rh/dec/PO_4 at 50 °C.

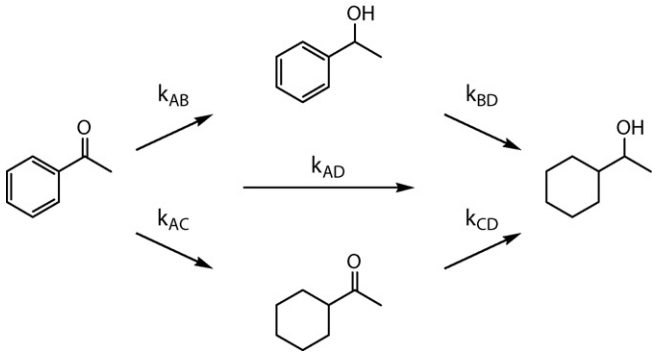

Fig. 5. Kinetic model for the reduction of acetophenone with supported catalysts.

reaction. Closer inspection of the concentration profiles during the initial phase of the reaction showed that 1-phenylethanol and 1-cyclohexylethanone were primary reaction products. The initial slope of zero in the concentration profile of 1-cyclohexylethanol indicates that this was a secondary product.

The reaction kinetics were modelled with the reaction sequence shown in Fig. 5 [45]. It was assumed that all reactions were first order in the reactants and essentially irreversible. Some reaction profiles could only be fitted, when the direct pathway from acetophenone to 1-cyclohexylethanol was included. This implies that both, phenyl and keto group, were reduced concurrently. Probably, the reaction intermediates (1-phenylethanol

Table 3
Conversion and selectivity in the hydrogenation of acetophenone with supported catalysts

Catalyst	Temperature (°C)	Time (h)	Conversion (%)	Selectivity[a] (%)	ee[b] (%)	Configuration[b]
Ru/dec/PO_4	50	15	22	35	49	*S*
Ru/tos/CO_3	50	17	36	19	55	*S*
Rh/dec/PO_4	30	30	95	41	13	*R*
Rh/dec/PO_4	50	15	90	70	30[c]	*R*
Rh/dec/PO_4	80	4	100	45	5	*R*
Rh/dbp/PO_4	30	29	20	58	19	*R*
Rh/tos/CO_3	50	22	100	6	74	*S*
Rh(chi)/tos/CO_3	50	24	63	38	2	*S*

[a] Chemoselectivity to 1-phenylethanol.
[b] Enantiomeric excess (ee) and configuration of 1-phenylethanol were determined by gas chromatography.
[c] 49% ee at 10% conversion.

Table 4
Rate constants for the hydrogenation of acetophenone with supported catalysts

Catalyst	Temperature (°C)	k_{AB} (h^{-1})	k_{AC} (h^{-1})	k_{BD} (h^{-1})	k_{CD} (h^{-1})	k_{AD} (h^{-1})	Ratio (k_{AB}/k_{AC})	Ratio $(k_{AB}+k_{CD})/(k_{AC}+k_{BD})$
Rh/dec/PO_4	30	0.064	0.038	0.018	0.043	0.006	1.7	1.9
Rh/dec/PO_4	50	0.169	0.046	0.008	0.065	0.005	3.7	4.3
Rh/dec/PO_4	80	0.678	0.177	0.062	0.038	0.299	3.8	3.0
Rh/dbp/PO_4	30	0.185	0.099	0	0.391	0.036	1.9	5.8
Rh/tos/CO_3	50	0.136	0.117	0.137	0.017	0	1.2	0.6
Ru/dec/PO_4[a]	50	0.108	0.109	0.100	0.012	0.045	1.0	0.6
Ru/tos/CO_3[a]	50	0.044	0.145	0	0.356	0.036	0.3	2.8

[a] Catalyst deactivation was taken into account.

and 1-cyclohexylethanone) remained coordinated to the metal centre, before diffusing from the ionic liquid into the hexane phase. Re-orientation of the substrate in the metal–substrate complex would be facilitated within a solvent cage (*vide infra*). However, it cannot be excluded that the intermediates were retained in the bulk ionic liquid phase and re-adsorbed at the metal centre.

The kinetic model provided a good fit for all catalysts employed in this study. Rate constants are given in Table 4. A good catalyst for the enantioselective reduction of acetophenone to 1-phenylethanol would have a high ratio k_{AB}/k_{AC}. A particularly high ratio k_{AB}/k_{AC} (3.7) was found for the catalyst Rh/dec/PO_4 in agreement with the high selectivity to 1-phenylethanol (70–73%). A more general measure for chemoselectivity to reduction of the keto-group is the ratio $(k_{AB}+k_{CD})/(k_{AC}+k_{BD})$, which was high for Rh/dec/PO_4 and Rh/dbp/PO_4 (4.3 and 5.8, respectively). Whether keto group or phenyl ring is reduced first depends on the coordination of the particular group to the metal centre and the relative rates of reduction [46]. The keto group can coordinate in σ or η^2-mode [47], whereas the phenyl ring can bind with one double bond (η^2) or with the whole π-system (η^6) [46]. An optimum catalyst for the regioselective synthesis of 1-phenylethanol would favour coordination of the keto group and bind phenyl rings only weakly and/or promote rapid reduction of the keto group while the phenyl ring reacts slowly. A catalyst for the synthesis of 1-cyclohexylethanol would provide a high rate for reduction of both keto group and phenyl ring. Note that in order to achieve enantioselectivity, simultaneous binding of keto and phenyl group to the metal centre is required (*vide infra*). Reduction of the phenyl ring was observed only for the supported catalysts, whereas high chemoselectivity to 1-phenylethanol was found in homogeneous catalysis.

Rate and selectivity of 1-phenylethanol formation were strongly dependent on temperature. With Rh/dec/PO_4, a maximum in selectivity to 1-phenylethanol was observed at 50 °C (70% at 90% conversion), while the selectivity was lower at 30 and 80 °C (56 and 43% at 90% conversion, respectively). Note that at lower temperatures (30 °C) the chemoselectivity to 1-phenylethanol decreased linearly with conversion (from 61 to 43%), which is typical for a consecutive reaction (Fig. 6). In contrast, the decrease in selectivity was very small at 50 °C (from 73 to 70%). At 80 °C, the selectivity was constant at 64% up to 80% conversion indicating that the products are formed

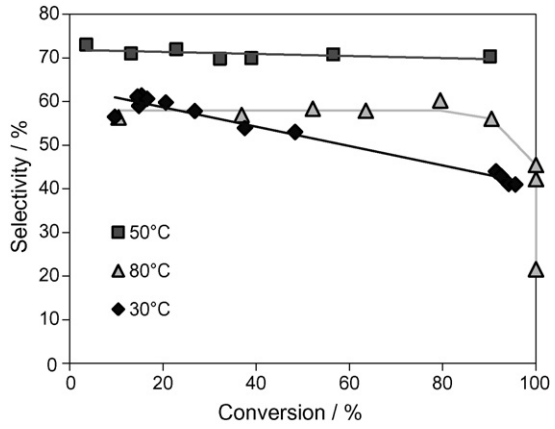

Fig. 6. Chemoselectivity to 1-phenylethanol vs. conversion in the hydrogenation of acetophenone with Rh/dec/PO_4.

by parallel reaction pathways. The temperature dependence is reflected in the ratio k_{AB}/k_{AC}, which increased from 1.7 at 30 °C to 3.7 at 50 °C (3.8 at 80 °C). The activation energy calculated for reaction AB (42 kJ mol^{-1}) was much higher than for reactions AC and BD (28 and 24 kJ mol^{-1}, respectively). The activation energy for reaction CD was close to zero. In contrast, the activation energy for reaction AD was particularly high (72 kJ mol^{-1}). The different energies of activation readily explain the observed maximum in chemoselectivity to 1-phenylethanol: at 30 °C, the influence of aromatic hydrogenation (k_{AC} and k_{BD}) was most pronounced, while the direct pathway to cyclohexylethanol (k_{AD}) was relevant only at high temperatures (80 °C). This is in agreement with the observed time-concentration profiles, which showed that 1-cyclohexylethanol was a secondary reaction product at low temperatures (low value of k_{AD}), while it was a primary reaction product at 80 °C.

To test for possible catalyst leaching, the reaction mixture was filtered after 2 h and hydrogenation was continued with the

Table 5
Homogeneous catalysts used in this study

Name	Organometallic complex	Additive
Rh/–/–	[Rh((*S*)-BINAP)(COD)]ClO_4·thf	–
Rh/–/CO_3	[Rh((*S*)-BINAP)(COD)]ClO_4·thf	K_2CO_3
Rh(chi)/–/CO_3	[Rh((*SS*)-chiraphos)(NOR)]ClO_4	K_2CO_3
Ru/–/CO_3	In situ mixture of $RuCl_3$ and (*R*)-BINAP	K_2CO_3

Table 6
Rate constants for the hydrogenation of acetophenone to 1-phenylethanol in homogeneous phase

Catalyst	Temperature (°C)	k_{AB} (h^{-1})	k_{AC} (h^{-1})	k_{BD} (h^{-1})	k_{CD} (h^{-1})	k_{AD} (h^{-1})	Time (h)	Conversion[a] (%)	Selectivity[b] (%)	ee (%)
Rh/–/–	50	–	–	–	–	–		0	–	–
Rh/–/CO_3	50	0.403	0	0	0	0	95	50	≥95	0
Rh(chi)/–/CO_3	50	0.057	0	0	0	0	40	47	≥96	0
Ru/–/CO_3	50	0.055	0.026	0.006	0.034	0	39	70	65	0

[a] Some catalyst deactivation was observed with all homogeneous catalysts.
[b] Chemoselectivity to 1-phenylethanol.

filtrate. Samples withdrawn after 5 and 15 h did not show further conversion. Thus, no catalytically active rhodium species leached into the hexane phase.

3.3. Comparison of supported and homogeneous catalysts

The performance of the supported catalysts was also compared with that of the corresponding homogeneous catalysts (Table 5). The homogeneous rhodium catalysts were highly selective for reduction of acetophenone to 1-phenylethanol. Only traces of by-products were observed in the final reaction mixtures. The catalytic activity of the supported rhodium catalysts was similar to the corresponding homogeneous catalysts (Table 6). For the complex [Rh((*S*)-BINAP)(COD)]ClO_4·thf, e.g., the initial rate of acetophenone consumption was 0.24 and 0.29 mol_{Sub} $(mol_{Cat}\ h)^{-1}$ for the supported (Rh/tos/CO_3) and homogenous catalyst (Rh/–/CO_3), respectively. No conversion was observed for the homogeneous catalysts, when K_2CO_3 was omitted from the reaction mixture. Clearly, basic reaction conditions were also essential similar to the supported catalysts. For ruthenium, the initial catalytic activity of the supported catalysts (0.24 and 0.21 mol_{Sub} $(mol_{Cat}\ h)^{-1}$ for Ru/dec/PO_4 and Ru/tos/CO_3, respectively) was considerably enhanced relative to the corresponding homogeneous catalyst [Ru((*R*)-BINAP)Cl_3] (Ru/–/CO_3, 0.08 mol_{Sub} $(mol_{Cat}\ h)^{-1}$).

While 74 and 30% ee were observed for Rh/tos/CO_3 and Rh/dec/PO_4, respectively, no enantioselectivity was observed for the corresponding homogeneous complex. This is particularly noteworthy as the effect of ionic liquid was also observed for the ruthenium catalysts and is indicative of a special mechanism of stereoselection. No enantioselectivity was observed with the homogeneous ruthenium complex in agreement with other studies, where 4% ee were reported using methanol as solvent [43]. In contrast, the corresponding supported catalysts Ru/dec/PO_4 and Ru/tos/CO_3 provided considerable enantioselectivity (49 and 55% ee, respectively).

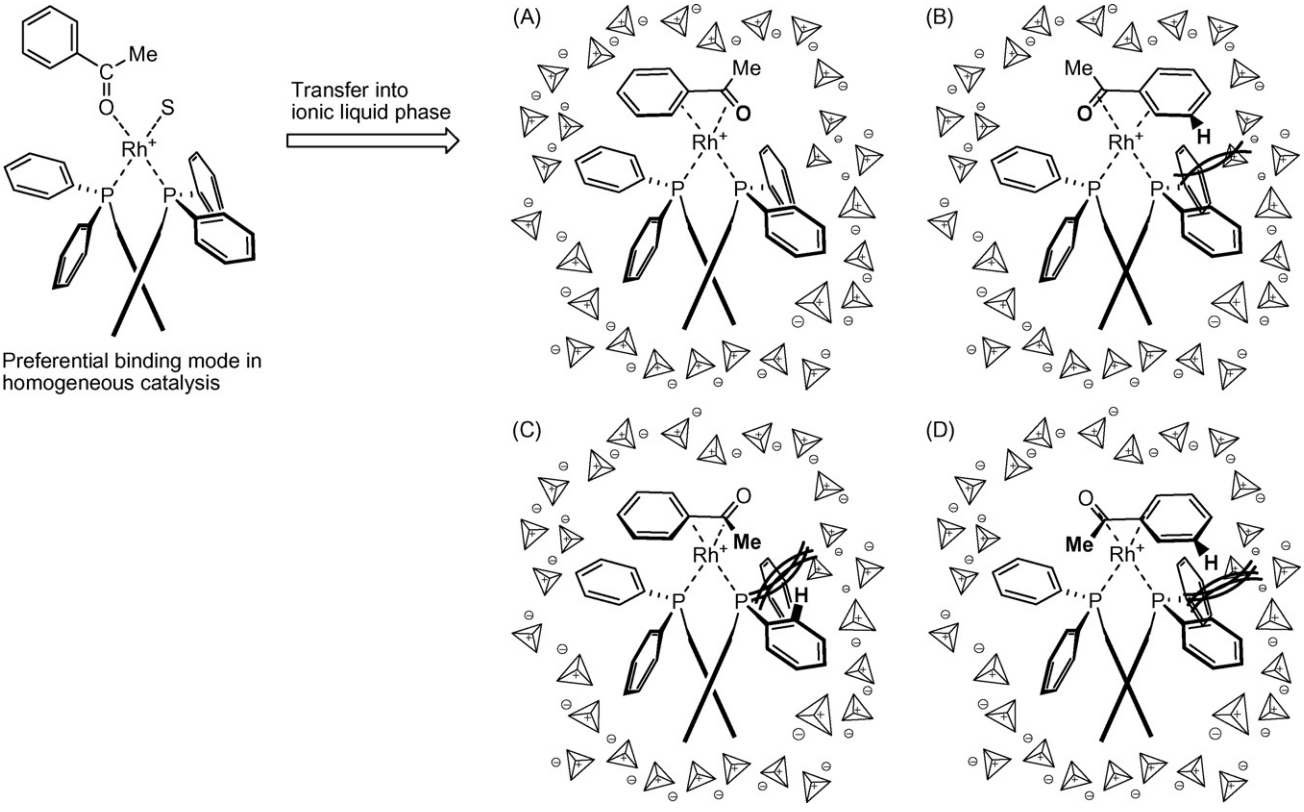

Scheme 1. Preferential coordination mode in homogenous catalysis and schematic representation of the geometry of the diastereomeric [Rh((*R*)-BINAP)(acetophenone)]$^+$ catalyst–substrate adduct in supported ionic liquids. A is the preferred coordination mode.

Apparently, the interactions between the acetophenone and the chiral phosphine ligand were enhanced in the ionic liquid. Note that the stereoselection was opposite for rhodium ((*R*)-BINAP providing (*R*)-1-phenylethanol) and ruthenium ((*R*)-BINAP providing (*S*)-1-phenylethanol).

3.4. Mechanism of enantioselectivity enhancement in supported ionic liquids

It is striking from literature that similar complexes as employed in this study generally provide low enantioselectivities in the reduction of aromatic ketones [38,43]. In contrast, ketones with a second binding group in the molecule can be reduced with high stereo-selectivities [32,38,39,48]. This suggests that the enhanced enantioselectivity observed here in reactions with supported catalysts in comparison to the corresponding homogeneous catalysis is a consequence of a different binding mode between substrate and metal complex.

In classic solvents, aromatic ketones are known to bind to rhodium and ruthenium preferentially *via* one of the free electron pairs of the oxygen atom [47]. The σ-coordination mode provides a large degree of flexibility for the ketone (Scheme 1). In consequence, stereoselective interactions between the BINAP ligand and the phenyl- or methyl group of acetophenone are weak. Alternatively, π-coordination (η^2) is possible [47], but also does not provide strong differentiation between the two faces.

We speculate that the solvent cages [24] formed around the metal-substrate complex in the ionic liquid phase of the supported catalysts are the key factor for the enhanced stereoselection. During dissolution of the metal complexes, inter-ionic interactions between the anions of the ionic liquid and the phosphonium cations are disrupted. In an attempt to minimize the potential energy, the sphere of ionic liquid molecules around the metal-substrate complex assumes a minimum size. Thereby, the substrate is squeezed against the metal, which leads to enhanced metal-substrate interactions. In consequence, simultaneous η^2/η^2-coordination of keto group and phenyl ring to the metal centre becomes possible.

A schematic representation of the preferential geometry of the diastereomeric [Rh((*R*)-BINAP)(acetophenone)]$^+$ catalyst-substrate adduct is shown in Scheme 1. In the η^2/η^2-coordination mode, acetophenone has to fit tightly into the pocket between the four phenyl groups of the BINAP ligand. The diastereomeric adduct A is clearly preferred, while repulsive steric interactions between the phenyl groups of the BINAP ligand and the phenyl and methyl group of acetophenone arise in the three alternative coordination modes B, C and D. Subsequent dissoziative coordination of hydrogen and transfer to the *si* face of acetophenone provides (*R*)-1-phenylethanol, in case of the (*R*)-BINAP rhodium complex.

4. Conclusions

Bifunctional supported catalysts comprising chiral rhodium or ruthenium complexes immobilised together with a base in thin films of phosphonium based ionic liquids were highly active catalysts for the enantioselective hydrogenation of acetophenone. The rate of reaction was generally similar or higher compared to the respective homogeneous catalysts. Reduction of the phenyl ring was observed as parallel or consecutive pathway leading to 1-cyclohexylethanol as the final product. This observation provided insight into mechanistic details. It is particularly noteworthy that high enantioselectivity (30–74%) was observed for catalyst/substrate pairs, where little chiral selection (≤4%) occurred in the corresponding homogeneous catalysis using methanol as solvent.

We speculate that substrate–catalyst interactions were enhanced in the supported catalysts. As in recent reports on imidazolium salts [24], the formation of solvent cages around the substrate–catalyst adducts was indicated by dramatic broadening of the NMR signals. Within the restricted space of the solvent cage, the preferred binding mode of acetophenone to the metal centre was concluded to be different from that in classic solvents such as methanol. A model is proposed, where acetophenone binds preferentially *via* both keto group and phenyl ring to the metal centre. Stereoselection is obtained, as the η^2/η^2-coordinated acetophenone has to fit tightly into the pocket formed by the phenyl rings of the chiral BINAP ligand.

The present study provides the first experimental evidence for the effect of the highly polar environment of an ionic liquid on enantioselection. We have established that simple rhodium complexes of the type [Rh(BINAP)L_2]X (L weakly coordinating ligand; X non-coordinating anion) are promising chiral catalysts for the enantioselective reduction of simple ketones, when immobilised together with a base in phosphonium based ionic liquids. Understanding the principles, on which this enhanced stereoselectivity is based, may provide inspiration for further studies using ionic liquids as reaction medium.

Acknowledgements

Lau Chau Sang and Yu Zhen performed parts of this study as UROPS project. BET surface area and metal contents of the catalysts were determined by Martin Neukamm. C, H, N analyses were measured by Dr. Barth and Mr. Tafelmaier, Mikroanalytisches Labor at TUM, Institut für Anorganische Chemie. Dr. Robertson from Cytec Industries Inc. and Dr. Hofmann from Degussa AG are thanked for providing ionic liquids and silica beads, respectively.

Appendix A. Supplementary data

Supplementary data associated with this article can be found, in the online version, at doi:10.1016/j.molcata.2006.11.050.

References

[1] C. Bolm, J.A. Gladysz, Chem. Rev. 103 (2003) 2761–2762.
[2] J. Mulzer, H. Waldmann, Organic Synthesis Highlights III, 3rd ed., Weinheim, 1998.
[3] A. Kirschning, Immobilized catalysts: solid phases, immobilization and applications, in: Topics in Current Chemistry, vol. 242, Springer, Berlin, 2004.

[4] D.E. De Vos, I.F.J. Vankelecom, P.A. Jacobs, Chiral Catalyst Immobilization and Recycling, Wiley-VCH, Weinheim, 2000.
[5] X. Wang, K. Ding, J. Am. Chem. Soc. 126 (2004) 10524–10525.
[6] Y. Liang, Q. Jing, X. Li, L. Shi, K. Ding, J. Am. Chem. Soc. 127 (2005) 7694–7695.
[7] C. Maillet, P. Janvier, M. Pipelier, T. Praveen, Y. Andres, B. Bujoli, Chem. Mater. 13 (2001) 2879–2884.
[8] A. Hu, H.L. Ngo, W. Lin, J. Am. Chem. Soc. 125 (2003) 11490–11491.
[9] K. Aoki, T. Shimada, T. Hayashi, Tetrahedron Asymmetry 15 (2004) 1771–1777.
[10] C.E. Song, S.-G. Lee, Chem. Rev. 102 (2002) 3495–3524.
[11] X. Li, W. Chen, W. Hems, F. King, J. Xiao, Org. Lett. 5 (2003) 4559–4561.
[12] B. Cornils, W.A. Herrmann, Aqueous-Phase Organometallic Catalysis, 2nd ed., Wiley-VCH, Weinheim, 2004.
[13] V. Neff, T.E. Müller, J.A. Lercher, J. Chem. Soc., Chem. Commun. 8 (2002) 906–907.
[14] H.L. Ngo, A. Hu, W. Lin, Tetrahedron Lett. 46 (2005) 595–597.
[15] D.Y. Murzin, P. Mäki-Arvela, E. Toukoniitty, T. Salmi, Catal. Rev. 47 (2005) 175–256.
[16] G.V. Smith, F. Notheisz, Heterogeneous Catalysis in Organic Chemistry, Academic Press, New York, 1999.
[17] S. Breitenlechner, M. Fleck, T.E. Müller, A. Suppan, J. Mol. Catal. A 214 (2004) 175–179.
[18] C.P. Mehnert, E.A. Cook, N.C. Dispenziere, M. Afeworki, J. Am. Chem. Soc. 124 (2002) 12932–12933.
[19] C.P. Mehnert, Chem. Eur. J. 11 (2005) 50–56.
[20] R.D. Rogers, K.R. Seddon, ACS Symposium Series, 818, American Chemical Society, Washington, 2002.
[21] M. Freemantle, C&EN (November 8, 2004) 44–49.
[22] T.J.S. Schubert, Nachrichten aus der Chemie 53 (2005) 1222–1226.
[23] N. Jain, A. Kumar, S. Chauhan, S.M.S. Chauhan, Tetrahedron 61 (2005) 1015–1060.
[24] C. Sievers, O. Jimenez, T.E. Müller, S. Steuernagel, J.A. Lercher, J. Am. Chem. Soc. 128 (2006) 13990–13991.
[25] R.E. Del Sesto, C. Corley, A. Robertson, J.S. Wilkes, J. Organomet. Chem. 690 (2005) 2536–2542.
[26] T. Ramnial, D.D. Ino, J.A.C. Clyburne, Chem. Commun. (2005) 325–327.
[27] J. Madec, X. Pfister, P. Phansavath, V. Ratovelomanana-Vidal, J.-P. Genet, Tetrahedron 57 (2001) 2563–2568.
[28] For an account on ruthenium catalysts, see:
J.-P. Genet, Acc. Chem. Res. 36 (2003) 908–918.
[29] H. Shimizu, I. Nagasaki, T. Saiko, Tetrahedron 61 (2005) 5405–5432.
[30] M. Berthod, G. Mignani, G. Woodward, M. Lemaire, Chem. Rev. 105 (2005) 1801–1836.
[31] S. Akutagawa, Appl. Catal. A 128 (1995) 171–207.
[32] T. Ohkuma, M. Koizumi, H. Doucet, T. Pham, M. Kozawa, K. Murata, E. Katayama, T. Yokozawa, T. Ikariya, R. Noyori, J. Am. Chem. Soc. 120 (1998) 13529–13530.
[33] J. Wu, H. Chen, W. Kwok, R. Guo, Z. Zhou, C. Yeung, A.S.C. Chan, J. Org. Chem. 67 (2002) 7908–7910.
[34] G.A. Grasa, A. Zanotti-Gerosa, J.A. Medlock, W.P. Hems, Org. Lett. 7 (2005) 1449–1451.
[35] T. Ohkuma, M. Koizumi, K. Muñiz, G. Hilt, C. Kabuto, R. Noyori, J. Am. Chem. Soc. 124 (2002) 6508–6509.
[36] H. Doucet, T. Ohkuma, K. Murata, T. Yokozawa, M. Kozawa, E. Katayama, A.F. England, T. Ikariya, R. Noyori, Angew. Chem. Int. Ed. 37 (1998) 1703–1707.
[37] PennPhos = P,P′-1,2-phenylenebis{2,5-dimethyl-7-phosphobicyclo[2.2.1]heptane}:
Q. Jiang, Y. Jiang, D. Xiao, P. Cao, X. Zhang, Angew. Chem. Int. Ed. 37 (1998) 1100–1103.
[38] T.T.-L. Au-Yeung, A.S.C. Chan, Coord. Chem. Rev. 248 (2004) 2151–2164.
[39] W. Tang, X. Zhang, Chem. Rev. 103 (2003) 3029–3069.
[40] A. Miyashita, A. Yasuda, H. Takaya, K. Toriumi, T. Ito, T. Souchi, R. Noyori, J. Am. Chem. Soc. 102 (1980) 7932–7934.
[41] D.D. Laws, H.-M.L. Bitter, A. Jerschow, Angew. Chem. Int. Ed. 41 (2002) 3096–3129 (and references cited therein).
[42] R. Spindler, D.F. Shriver, J. Am. Chem. Soc. 110 (1998) 3036–3043.
[43] U. Matteoli, V. Beghetto, A. Scrivanti, J. Mol. Catal. A Chem. 140 (1999) 131–137.
[44] R. Noyori, T. Ohkuma, Angew. Chem. Int. Ed. 40 (2001) 40–73.
[45] P. Tundo, S. Zinovyev, A. Perosa, J. Catal. 196 (2000) 330–338.
[46] J.P. Collman, L.S. Hegedus, J.R. Norton, R.G. Finke, Principles and Applications of Organotransition Metal Chemistry, United Science Books, Mill Valley, 1987.
[47] R. Noyori, M. Yamakawa, S. Hashiguchi, J. Org. Chem. 66 (2001) 7931–7944.
[48] H. Doucet, P. Le Gendre, C. Bruneau, P.H. Dixneuf, J.C. Souvie, Tetrahedron: Asymmetry 7 (1996) 525–528.